Theor Chim Acta (1993) 85: 17–26

Theoretica Chimica Acta

Molecular orbital studies on nucleoside antibiotics X. Conformation of nebularine and isoguanosine

A. Saran and L. N. Patnaik*

Chemical Physics Group, Tata Institute of Fundamental Research, Homi Bhabha Road, Bombay 400 005, India

Received August 10, 1991/Accepted October 18, 1991

Summary. Conformational properties of two nucleoside analogs, namely nebularine and isoguanosine have been investigated by using PCILO (Perturbative Configuration Interaction using Localized Orbitals) method. Nebularine (9-β-ribofurnosyl purine) is a naturally occurring purine nucleoside which is structurally similar to adenosine and it inhibits the growth of tumor cells and influenza B virus. Isoguanosine is one of the two naturally occurring analogs of guanosine. Both C2′-*endo* and C3′-*endo* sugar puckerings have been considered for both the molecules with preselected values of torsion angles around C2′–O2′ and C5′–O5′ bonds. The results indicate that nebularine has conformational preferences very similar to those of its parent nucleoside, adenosine; whereas the conformational properties of isoguanosine are very different from those of guanosine as well as adenosine. The important implications of these results have been discussed in terms of the biological activity of these molecules.

Key words: Nebularine – Isoguanosine – Crotonoside – PCILO – Conformation – Nucleoside antibiotics

1. Introduction

It is a great pleasure to contribute to this volume in honor of Prof. (Mme.) Alberte Pullman. In fact, one of us (A.S.) had the privilege of working in Prof. Pullman's group in Paris several years ago.

Minor modifications or substitutions either in the sugar or in the base part of nucleosides result in a class of biologically important molecules known as nucleoside antibiotics. These antibiotics exhibit a variety of antiviral, antibacterial, antitumor and cancerostatic activities [1–3]. We have been interested in the conformation of these antibiotics in recent years by using quantum-mechanical PCILO method with an aim to understand the mechanism of their action [4–13]; the results of our studies have established a strong correlation between the conformation and the biological activity of these molecules [14, 15]. The present

* *Permanent address*: State Prevention and Control of Pollution Board, Bhubaneswar 751 012, India

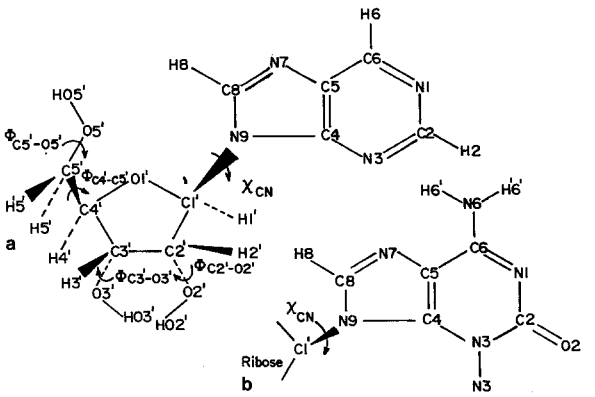

Fig. 1. Torsion angles involved in (**a**) nebularine and (**b**) isoguanosine

investigation reports the results of a similar study on two such modified nucleosides, namely, nebularine and isoguanosine.

Nebularine, a naturally occurring nucleoside antibiotic, is structurally similar to adenosine with the exception that the $-NH_2$ group attached to the C6 atom in adenosine is replaced by a proton in nebularine (Fig. 1a). It is isolated from the mushroom *Agaricus* (*Clitocybe*) *nebularis batsch* and from *Streptomyces yokosukanensis* and is toxic to mice, *mycobacterium* and animal cells in culture and inhibits tumor growth [2, 3]. Isoguanosine (crotonoside shown in Fig. 1b) was first isolated from the seeds of *Croton tiglium* L. and is not strictly a nucleoside antibiotic [2]. Isoguanosine and 2′-amino-2′-deoxyguanosine are the only two naturally occurring analogs of guanosine [2, 3]. We have studied the conformational properties of 2′-amino-2′-deoxyguanosine and compared them to those of its parent nucleoside [11]. It is, therefore, a worthwhile interesting exercise to extend a similar study to isoguanosine, the other analog of guanosine and compare its results with those of 2′-amino-2′-deoxyguanosine and guanosine. The results of these studies are presented in this paper.

2. Procedure

The essential features of PCILO formalism [16, 17] are described in [18, 19]. The various torsion angles (Fig. 1) which determine the conformation of the molecules are: χ_{CN} [20]. $\phi_{C2'-O2'}$, $\phi_{C3'-O3'}$, $\phi_{C4'-C5'}$ and $\phi_{C5'-O5'}$ [18, 21] and these are defined as:

$$\chi_{CN} = O1'-C1'-N9-C8$$

$$\phi_{C2'-O2'} = C1'-C2'-O2'-HO2'$$

$$\phi_{C3'-O3'} = C2'-C3'-O3'-HO3'$$

$$\phi_{C4'-C5'} = C3'-C4'-C5'-O5' \quad \text{and}$$

$$\phi_{C5'-O5'} = C4'-C5'-O5'-HO5'.$$

The torsion angle corresponding to the *cis*-planar arrangement of the terminal bonds is taken as zero. The values of $\chi_{CN} = 0° \pm 90°$ and $180° \pm 90°$, correspond, respectively, to the *anti* and *syn* regions of glycosyl torsion angle

[20]. The *gg*, *gt* and *tg* conformation around the exocyclic C4′–C5′ bond correspond to $\phi_{C4'-C5'} = 60°$, 180° and 300°, respectively.

The input geometrical data (bond lengths and bond angles) for C3′-*endo* nebularine have been adopted from its crystal structure [22], while for C2′-*endo* nebularine, the sugar geometry has been taken from the standard values [23]. For isoguanosine, the base geometry has been adopted from the crystallographic data [24], while both the C2′-*endo* and C3′-*endo* geometrics for the sugar moiety have been taken from the standard values [23]. It is relevant here to mention that in the crystallographic studies of isoguanosine cation [24], both N1 and N7 atoms are protonated. We have, however, carried out computations on unprotonated isoguanosine (see Fig. 1).

PCILO energies have been computed as a function of torsion angles χ_{CN} and $\phi_{C4'-C5'}$ at 30° intervals of the torsion angles with preselected values of $\phi_{C2'-O2'}$ and $\phi_{C5'-O5'}$. The preselected values of these torsion angles allow or disallow the possibility of intramolecular hydrogen bonding between the sugar and the base. For C2′-*endo* sugar geometry, there are two possibilities of intramolecular hydrogen bonding:

(i) between O5′–HO5′ of the sugar and N3 of the base with the condition: $\phi_{C4'-C5'} = 60°$ and $\phi_{C5'-O5'} = 60°$ and 300° and

(ii) between O2′–HO2′ of the sugar and N3 of the base with the condition: $\phi_{C2'-O2'} = 60°$.

In the first case HO5′ orients towards the base, while in the second HO2′ orients towards the base. The values of torsion angles $\phi_{C5'-O5'} = 180°$ and $\phi_{C2'-O2'} = 180°$, orient HO5′ and HO2′ away from the base and thus, prevents any possibility of intramolecular hydrogen bonding. For C3′-*endo* sugar geometry, the second possibility viz. O2′–HO2′ ··· N3 hydrogen bonding is not possible as the participating atoms in the hydrogen bonding are farther apart than in the case of C2′-*endo* sugar geometry [4, 7, 8]. Two-dimensional conformational energy maps in $(\chi_{CN} - \phi_{C4'-C5'})$ hyper-space have been constructed by limiting the isoenergy curves upto 5 kcal/mol above the global minimum. In all, twenty such conformational energy maps have been constructed for both molecules, ten maps for each with the two C2′-*endo* and C3′-*endo* sugar geometries. The preselected values of torsion angles are: $\phi_{C5'-O5'} = 60°$, 180° and 300° with $\phi_{C2'-O2'} = 180°$ and $\phi_{C5'-O5'} = 60°$ and 180° with $\phi_{C2'-O2'} = 60°$. The value of $\phi_{C3'-O3'}$ has been kept fixed at 180° in all the computations. The results of all the maps are discussed below.

3. Results and discussion

The global minima as well as the low energy regions upto 1 kcal/mol for both the molecules have been recorded in Tables 1 and 2 with their energies by taking the lowest global minimum of each molecule as energy zero.

3.1. C2′-endo nebularine

Figure 2 shows the most stable map for C2′-*endo* nebularine which has been obtained with preselection: $\phi_{C2'-O2'} = 60°$ and $\phi_{C5'-O5'} = 180°$. It can be seen

from this map that the global minimum occurs at $\chi_{CN} = 330°$ (*anti*) and $\phi_{C4'-C5'} = 60°$ (*gg*) which is stabilized due to intramolecular hydrogen bonding between O2′ of the sugar and N3 of the base through favorable orientation of HO2′ as discussed in the previous section. The low energy region associated with the global minimum extends from $\phi_{C4'-C5'} = 30°$ to 90°. Similar conformational features have also been observed in our earlier studies [6, 7, 24].

The next stable map is the one obtained with $\phi_{C2'-O2'} = 180°$ and $\phi_{C5'-O5'} = 60°$. This map is shown in Fig. 3, and it can be observed that a highly localized global minimum occurs at $\chi_{CN} = 210°$ (*syn*) and $\phi_{C4'-C5'} = 60°$. This global minimum is, again, due to strong intramolecular hydrogen bonding between O5′–HO5′ of the sugar and N3 of the base. However, this minimum is about 0.5 kcal/mol higher in energy than that of Fig. 2 (see Table 1).

The next stable map is obtained with the preselection $\phi_{C2'-O2'} = \phi_{C5'-O5'} = 60°$ (see Table 1). In this preselection both HO2′ and HO5′ are oriented towards the base and they are capable of forming intramolecular hydrogen bonds with N3. One, therefore, expects all the conformational features of Figs. 2 and 3 in the conformational energy map and indeed these are seen in Fig. 4. In the ensuing competition, the hydrogen bond involving HO5′ predominates over that involving HO2′ and the global minimum occurs at $\chi_{CN} = 210°$ (*syn*) and $\phi_{C4'-C5'} = 60°$ (*gg*), whereas the minimum at $\chi_{CN} = 330°$ (*anti*) and $\phi_{C4'-C5'} = 60°$ (*gg*) is about 1 kcal/mol above the global minimum.

It is clear from Table 1 that the map constructed with $\phi_{C2'-O2'} = 180°$ and $\phi_{C5'-O5'} = 300°$ has the global minimum at $\chi_{CN} = 240°$ (*syn*) and $\phi_{C4'-C5'} = 120°$. This minimum is about 3.2 kcal/mol higher in energy than the most stable conformation shown in Fig. 2.

Figure 5 shows the conformational energy map which has been constructed for C2′-*endo* nebularine with $\phi_{C2'-O2'} = \phi_{C5'-O5'} = 180°$. In this preselection both HO2′ and HO5′ are oriented away from the base and there is no possibility

Table 1. Preferred conformations of nebularine by the PCILO method

Sugar pucker	Conformational map		Global minimum			Low energy regions		
	$\phi_{C2'-O2'}$	$\phi_{C5'-O5'}$	χ_{CN}	$\phi_{C4'-C5'}$	Energy[a]	χ_{CN}	$\phi_{C4'-C5'}$	Energy[a]
	60	180	330 (*anti*)	60 (*gg*)	0.0			
	180	60	210 (*syn*)	60 (*gg*)	0.5			
C2′-*endo*	60	60	210 (*syn*)	60 (*gg*)	1.0	330 (*anti*)	60 (*gg*)	2.0
	180	300	240 (*syn*)	120	3.2	210 (*syn*)	150 (*gt*)	3.7
	180	180	300 (*anti*)	60 (*gg*)	6.7	60 (*anti*)	60 (*gg*)	7.2
						270	180 (*gt*)	7.7
						270	300 (*gt*)	7.7
	180	60	180 (*syn*)	30 (*gg*)	0.0	330 (*anti*)	60 (*gg*)	1.0
	180	180	330 (*anti*)	60 (*gg*)	0.7	330 (*anti*)	300 (*tg*)	1.7
C3′-*endo*	180	300	240 (*syn*)	90 (*gg*)	0.9	180 (*syn*)	150 (*gt*)	1.4
	60	60	180 (*syn*)	30 (*gg*)	1.6	330 (*anti*)	60 (*gg*)	2.6
	60	180	330 (*anti*)	60 (*gg*)	2.5	330 (*anti*)	300 (*tg*)	3.5

[a] Energy in kcal/mol by taking the lowest global minimum energy of each molecule as energy zero. Torsion angles are in degrees.

of any intramolecular hydrogen bonding between the sugar and the base. The global minimum occurs at $\chi_{CN} = 300°$ (*anti*) and $\phi_{C4'-C5'} = 60°$ (*gg*) with a local minimum above 0.5 kcal/mol higher in energy at $\chi_{CN} = 60°$ (*anti*) and $\phi_{C4'-C5'} = 60°$ (*gg*). The conformational flexibility is much larger in this map than that in the maps of Figs 2-4 and both *anti* and *syn* regions of χ_{CN} are within 2 kcal/mol above the global minimum. In addition to these, there are two low energy regions within 1 kcal/mol at $\chi_{CN} = 270°$ (*anti*) and associated with $\phi_{C4'-C5'} = 180°$ (*gt*) and 300° (*tg*). Energetically the global minimum this map (Fig. 5) is about 6.7 kcal/mol higher in energy than that of the most stable map shown in Fig. 2.

3.2. C3-*endo* nebularine

Figure 6 shows the most stable conformational map for C3′-*endo* nebularine which has been obtained with preselection: $\phi_{C2'-O2'} = 180°$ and $\phi_{C5'-O5'} = 60°$ and the global minimum occurs at $\chi_{CN} = 180°$ (*syn*) and $\phi_{C4'-C5'} = 30°$ (*gg*). This global minimum is stabilized due to intramolecular hydrogen bonding between O5′–HO5′ and N3. There is a low energy region about 1 kcal/mol higher in energy at $\chi_{CN} = 330°$ (*anti*) and $\phi_{C4'-C5'} = 60°$ (*gg*) but the *anti* and *syn* regions are separated by large barrier heights between them.

The next stable map is the one which has been constructed with the preselection $\phi_{C2'-O2'} = \phi_{C5'-O5'} = 180°$. This map shown in Fig. 7 again shows large conformational flexibility similar to that of the map in Fig. 5. The global minimum occurs at $\chi_{CN} = 330°$ (*anti*) and $\phi_{C4'-C5'} = 60°$ (*gg*) and the low energy regions surrounding the global minimum extends from $\chi_{CN} = 315°$ to 15° in the *anti* region. The *syn* regions ($\chi_{CN} \approx 180°$) is about 2 kcal/mol higher in energy and are separated from *anti* regions by a barrier height of 3 kcal/mol. There is a low energy region about 1 kcal/mol higher in energy at $\chi_{CN} = 330°$ (*anti*) and $\phi_{C4'-C5'} = 300°$ (*tg*).

It can be seen from Table 1 that the global minimum of the map constructed with $\phi_{C2'-O2'} = 180°$ and $\phi_{C5'-O5'} = 300°$ occurs at $\chi_{CN} = 240°$ (*syn*) and $\phi_{C4'-C5'} = 90°$ (*gg*). This global minimum is stabilized again due to intramolecular hydrogen bonding between O5′ and N3 through HO5′. Besides this, there is a low energy region about 0.5 kcal/mol higher in energy at $\chi_{CN} = 180°$ (*syn*) and $\phi_{C4'-C5'} = 150°$ (*gt*). The next two conformational energy maps have been constructed with $\phi_{C2'-O2'} = 60°$ and $\phi_{C5'-O5'} = 60°$ and 180° and their conformational features similar to those observed in Figs. 6 and 7. Table 1 shows the global minimum for the map with $\phi_{C5'-O5'} = 60°$ at $\chi_{CN} = 180°$ (*syn*) and $\phi_{C4'-C5'} = 30°$ (*gg*), while for the map with $\phi_{C5'-O5'} = 180°$ it is at $\chi_{CN} = 330°$ (*anti*) and $\phi_{C4'-C5'} = 60°$ (*gg*). The low energy regions in these two maps are recorded in Table 1.

3.3. C2′-*endo* isoguanosine

Figure 8 shows the conformational energy map constructed for C2′-*endo* isoguanosine with preselection: $\phi_{C2'-O2'} = \phi_{C5'-O5'} = 180°$. The global minimum occurs at $\chi_{CN} = 240°$ (*syn*) and $\phi_{C4'-C5'} = 60°$ (*gg*). It can be seen from this map that there is considerable conformational flexibility. In fact, the remaining four

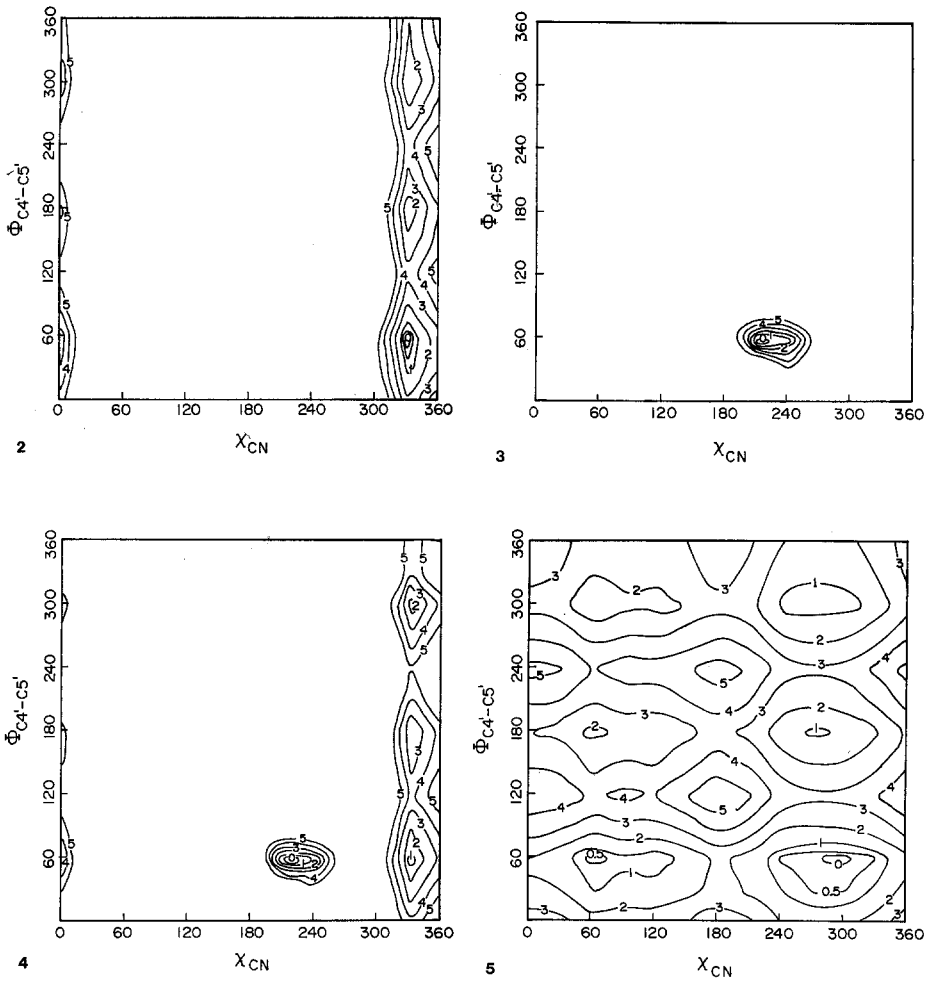

Fig. 2. ($\chi_{CN} - \phi_{C4'-C5'}$) conformational energy map for C2′-*endo* nebularine with $\phi_{C2'-O2'} = 60°$ and $\phi_{C5'-O5'} = 180°$. Isoenergy curves in kcal/mol by taking the global minimum as energy zero

Fig. 3. ($\chi_{CN} - \phi_{C4'-C5'}$) conformational energy map for C2′-*endo* nebularine with $\phi_{C2'-O2'} = 180°$ and $\phi_{C5'-O5'} = 60°$. Isoenergy curves in kcal/mol by taking the global minimum as energy zero

Fig. 4. ($\chi_{CN} - \phi_{C4'-C5'}$) conformational energy map for C2′-*endo* nebularine with $\phi_{C2'-O2'} = \phi_{C5'-O5'} = 60°$. Isoenergy curves in kcal/mol by taking the global minimum as energy zero

Fig. 5. ($\chi_{CN} - \phi_{C4'-C5'}$) conformational energy map for C2′-*endo* nebularine with $\phi_{C2'-O2'} = \phi_{C5'-O5'} = 180°$. Isoenergy curves in kcal/mol by taking the global minimum as energy zero

maps also exhibit large conformational flexibility. However, the map constructed with $\phi_{C2'-O2'} = 60°$ and $\phi_{C5'-O5'} = 180°$ has similar conformational features to those of the map shown in Fig. 8 with the exception of energy contours associated with $\chi_{CN} = 330°$ through the whole region of $\phi_{C4'-C5'}$ The third and fourth maps again show similar conformational features. Both maps constructed with $\phi_{C2'-O2'} = 180$

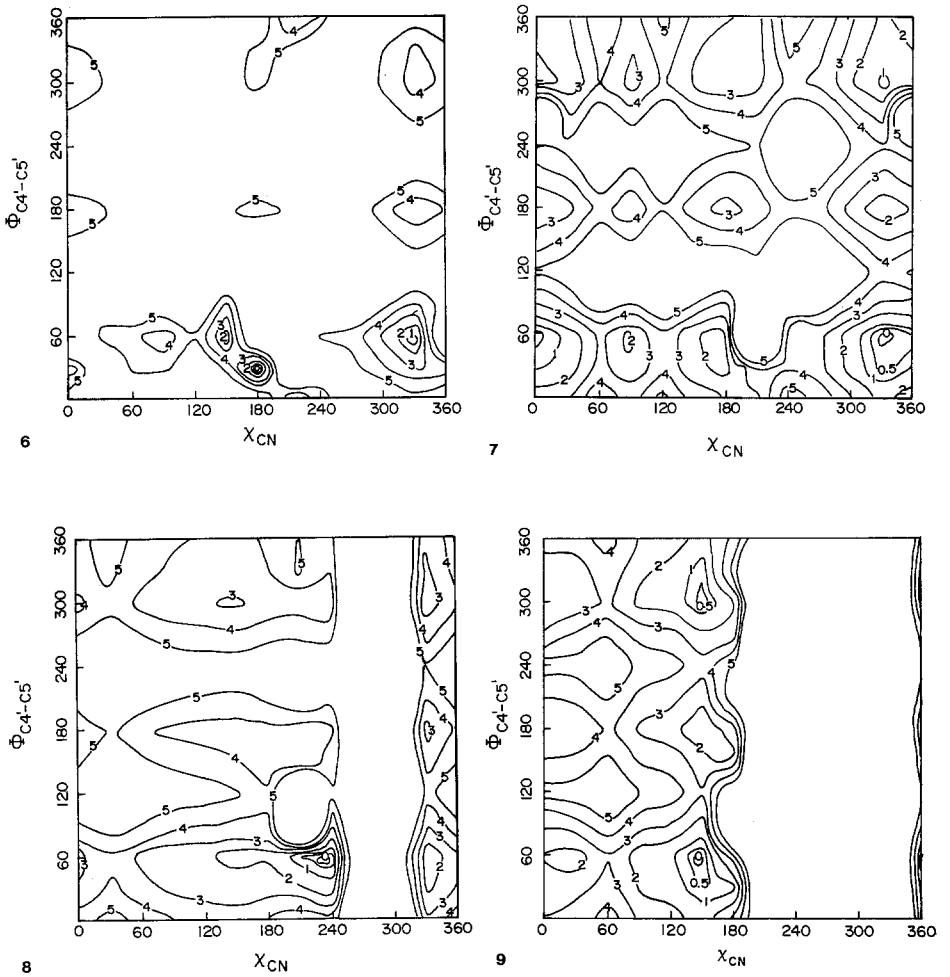

Fig. 6. ($\chi_{CN} - \phi_{C4'-C5'}$) conformational energy map for C3′-*endo* nebularine with $\phi_{C2'-O2'} = 180°$ and $\phi_{C5'-O5'} = 60°$. Isoenergy curves in kcal/mol by taking the global minimum as energy zero

Fig. 7. ($\chi_{CN} - \phi_{C4'-C5'}$) conformational energy map for C3′-*endo* nebularine with $\phi_{C2'-O2'} = \phi_{C5'-O5'} = 180°$. Isoenergy curves in kcal/mol by taking the global minimum as energy zero

Fig. 8. ($\chi_{CN} - \phi_{C4'-C5'}$) conformational energy map for C2′-*endo* isoguanosine with $\phi_{C2'-O2'} = \phi_{C5'-O5'} = 180°$. Isoenergy curves in kcal/mol by taking the global minimum as energy zero

Fig. 9. ($\chi_{CN} - \phi_{C4'-C5'}$) conformational energy map for C3′-*endo* isoguanosine with $\phi_{C2'-O2'} = \phi_{C5'-O5'} = 180°$. Isoenergy curves in kcal/mol by taking the global minimum as energy zero

and $\phi_{C5'-O5'} = 60°$ and 300° shows the global minimum at $\chi_{CN} = 330°$ (*anti*) but associated with $\phi_{C4'-C5'} = 60°$ (*gg*) in the third and with $\phi_{C4'-C5'} = 180°$ (*gt*) in the fourth map (see Table 2). The fifth map is similar to the second map with the exception that the global minimum occurs at $\chi_{CN} = 180°$ (*syn*) and $\phi_{C4'-C5'} = 60°$. The low energy regions of all the five maps are recorded in Table 2.

Table 2. Preferred conformations of isoguanosine by the PCILO method

Sugar pucker	Conformational map		Global minimum			Low energy regions		
	$\phi_{C2'-O2'}$	$\phi_{C5'-O5'}$	χ_{CN}	$\phi_{C4'-C5'}$	Energy[a]	χ_{CN}	$\phi_{C4'-C5'}$	Energy[a]
	180	180	240 (*syn*)	60 (*gg*)	0.0			
	60	180	240 (*syn*)	60 (*gg*)	0.9			
C2′-*endo*	180	60	330 (*anti*)	60 (*gg*)	3.2	60–180	60 (*gg*)	4.2
						330 (*anti*)	300 (*gt*)	4.2
	180	300	330 (*anti*)	180 (*gt*)	3.7	210 (*syn*)	60 (*gg*)	4.2
						330 (*anti*)	60 (*gg*)	4.2
						330 (*anti*)	300 (*tg*)	4.7
						150 (*syn*)	180 (*gt*)	4.7
	60	60	150–180 (*syn*)	60 (*gg*)	3.9	60 (*anti*)	60 (*gg*)	4.9
						150 (*syn*)	300 (*tg*)	4.9
	180	60	150 (*syn*)	60 (*gg*)	0.0			
	180	180	150 (*syn*)	60 (*gg*)	0.2	150 (*syn*)	300 (*tg*)	0.7
						150 (*syn*)	330 (*tg*)	1.2
C3′-*endo*	60	60	150 (*syn*)	60 (*gg*)	2.4			
	180	300	150 (*syn*)	300 (*tg*)	2.5	150 (*syn*)	180 (*gt*)	2.7
						150 (*syn*)	60 (*gg*)	2.7
	60	180	150 (*syn*)	60 (*gg*)	2.6	150 (*syn*)	330 (*tg*)	3.6

[a] Energy in kcal/mol by taking the lowest global minimum energy of each molecule as energy zero. Torsion angles are in degrees.

3.4. C3′-*endo isoguanosine*

Table 2 indicates that the conformational energy maps constructed for C3′-*endo* isoguanosine with $\phi_{C2'-O2'} = 180°$ and $\phi_{C5'-O5'} = 60°$ and 180° have global minimum at $\chi_{CN} = 150°$ (*syn*) and $\phi_{C4'-C5'} = 60°$ (*gg*). Both maps are quite similar to each other but conformational flexibility is large in the second map (Fig. 9) as compared to the first map. Further, the difference in the global minimum energy between the two maps is only about 0.2 kcal/mol. This is due to the fact that there is no intramolecular hydrogen bonding between O5′–HO5′ of the sugar and N of the base because there is a proton attached of N3 (see Fig. 1b) in isoguanosine. In fact, one can see from Table 2 that the conformational features of all the five maps of isoguanosine are similar with exception of the fourth maps in which the global minimum shifts from $\chi_{CN} = 150°$ (*syn*) and $\phi_{C4'-C5'} = 60°$ (*gg*) to $\chi_{CN} = 150°$ (*syn*) and $\phi_{C4'-C5'} = 300°$ (*tg*). The low energy regions are recorded in Table 2.

4. Biological significance

On comparison of PCILO results on the conformation of nebularine with those of adenosine [22, 26], one finds that both have very similar conformational preferences. For the C2′-*endo* sugar pucker, where intramolecular hydrogen

bonding through HO2′ is allowed, both molecules prefer *anti* conformation for χ_{CN} and *gg* conformation for $\chi_{C4'-C5'}$. On the other hand, when intramolecular hydrogen bonding through HO5′ is allowed, both molecules prefer *syn–gg* conformation having either of the sugar puckers. However, when no intramolecular hydrogen bonding between sugar and base is allowed (i.e. $\phi_{C2'-O2'} = \phi_{C5'-O5'} = 180°$) both molecules show striking similarity in conformational preferences having large conformational flexibility with low energy barriers between *anti* and *syn* regions associated with *gg* conformation. Similar results have been obtained in our earlier PCILO studies on toyocamycin, sangivamycin, cordycepin, and 3′-deoxy-3′-aminoadenosine [6, 8]. The above-mentioned similarity assumes important biological significance because the conformational features obtained with $\phi_{C2'-O2'} = \phi_{C5'-O5'} = 180°$ are very similar to those prevailing in aqueous medium. In this preselection, as mentioned earlier, both HO2′ and HO5′ are oriented away from the base and no intramolecular hydrogen bonding is possible and this is the situation that prevails in biological environment which is predominantly aqueous. This is due to the fact that the two potential hydrogen bonding sites will be solvated by two water molecules through two intermolecular hydrogen bonds rather involved in one intramolecular hydrogen bond. This hypothesis has been fully corroborated by excellent agreement between theoretical and experimental NMR, ORD and CD results on a number of biologically active compounds: 6-azauridine and 6-azacytidine [4], tubercidin [5], cordycepin [8], and propranolol: a β-blocking adrenergic drug [27]. The experimental evidence in all the cases indicates an open structure for the molecules without any intramolecular hydrogen bond. Therefore, because of the striking conformational similarity in aqueous medium with adenosine, nebularine can successfuly mimick adenosine in biological reactions and this is indeed so. In the presence of adenosine kinase, nebularine is readily phosphorylated and inhibits RNA and DNA syntheses and thus, becomes cytotoxic [2].

The preferred conformations of isoguanosine, on the other hand, are totally different from those of either adenosine [24, 25] or guanosine or 2′-amino-2′-deoxyguanosine [11] in all the cases whether the intramolecular hydrogen bonding possibility is allowed or disallowed. As a consequence of this, isoguanosine can not mimick adenosine or guanosine and is, therefore, biologically inactive. Experimentally, it has been observed that isoguanosine can not serve as a sole source of purine in the growth of *Lactobacillus casei* nor is it incorporated into mammalian nucleic acids [2].

5. Conclusions

In conclusion, our present results on nebularine indicates that their conformational preferences are very similar to those of its parent nucleoside adenosine; whereas the conformational preferences of isoguanosine are completely different from those of either adenosine or guanosine. These results, further, confirms the correlation which we have obtained on the biological activity of a number of nucleoside antibiotics [14, 15]. It should be underlined here that the results on isoguanosine demonstrate that the converse of the correlation is also true. Similar conclusion about the validity of the converse of the correlation has also been demonstrated in our earlier studies on the conformation of 3-deazadenosine and 3-deazaguanosine [28].

References

1. Bloch A (1975) Ann NY Acad Sci 255:576
2. Suhadolnik RJ (1970) Nucleoside antibiotics. Wiley, NY
3. Suhadolnik RJ (1979) Nucleosides as biological probes. Wiley, NY
4. Mitra C, Saran A (1978) Biochim Biophys Acta 518:193
5. Saran A, Mitra C (1979) Indian J Biochem Biophys 16:304
6. Saran A, Chatterjee CL (1980) Int J Quantum Chem QBS 7:123
7. Saran A, Chatterjee CL (1980) Biochim Biophys Acta 607: 490
8. Saran A, Patnaik LN (1981) Int J Quantum Chem 20:357
9. Saran A, Chatterjee CL (1981) Int J Quantum Chem QBS 8:129
10. Saran A, Patnaik LN (1982) Int J Quantum Chem QBS 9:247
11. Patnaik LN, Saran A (1984) J Biol Phys 12:12
12. Saran A, Patnaik LN (1986) Int Quantum Chem OBS 13:121
13. Saran A (1988) J Mol Struct (Theochem) 189:215
14. Saran A (1987) Proc Indian Acad Sci Chem Sci 99:119
15. Saran A (1989), Int J Quantum Chem 35:193
16. Diner S, Malrieu JP, Claverie P (1969) Theor Chim Acta 13:1
17. Jordan F, Gilbert M, Malrieu JP, Pincilli U (1971) Theor Chim Acta 15:211 and references quoted therein
18. Pullman B, Saran A (1976) Proc Nuc Acid Res Mol Biol 16:215
19. Sundaralingam M (1969) Biopolymers 6:821
20. Saran A, Pullman B, Perahia D (1972) Biochim Biophys Acta 287:211
21. Takeda T, Ohashi Y, Sasada Y (1974) Acta Crystallogr B30:825
22. Arnott S, Huckins DWL (1972) Biochem J 130:453
23. Subramanian E, Marsh RE (1971) Acta Crystallogr B27:753
24. Saran A, Mitra C, Pullman B (1978) Biochim Biophys Acta 517:255
25. Berthod H, Pullman B (1971) Biochim Biophys Acta 232:595
26. Pullman B, Berthod H (1973) in: Bergmann E, Pullman B (eds) Conformation of biological molecules and polymers. Proc 5th Jerusalem Symp. Academic Press, NY p 209
27. Kulkarni VM, Vasanthkumar N, Saran A, Govil G (1979) Int J Quantum Chem QBS 6:153
28. Saran A, Chatterjee CL (1984) Int J Quantum Chem 25:743